MARTIAN HYDROTHERMAL SYSTEMS: RELATIONSHIP BETWEEN MAGNETIC ANOMALIES AND VALLEY NETWORKS K. P. Harrison[1] and R. E. Grimm[1,2], [1]Laboratory for Atmospheric and Space Physics, University of Colorado, Campus Box 392, Boulder, Colorado 80303, keith.harrison@colorado.edu, [2]Blackhawk Geoservices, Inc., 301 B Commercial Rd., Golden, Colorado 80401, grimm@blackhawkgeo.com.

Introduction: Regions of Mars containing high densities of valley networks [1] broadly correlate with zones of concentrated magnetic anomalies [2] and inferred crustal magnetism (Fig. 1). Such a correlation suggests a link between processes involving the acquisition of thermoremanance in a cooling intrusion and processes involving the production of surface water for the creation of fluvial channels. Hydrothermal circulation may control both processes. Numerical models show that the cumulative water discharge due to intrusions building a column of crust spans a comparable range as the inferred discharge from valley networks over the crustal column and its hydrothermal system.

Our hypothesis is developed by considering (1) formation of the magnetic anomalies as intruded crust, including the acquisition of thermoremanance at relatively great depth, (2) numerically modeling the linked thermal evolution of cooling magma bodies and their attendant hydrothermal systems, and (3) comparing the hydrothermal discharge to that estimated from valley-network morphology.

Crustal Magnetism: Under either limited lateral spreading or serial vertical intrusion, the southern highlands crust of Mars must have accumulated as a series of magmatic intrusions at various depths. Strong magnetization of 20-40 Am^2 [3,4] implies that the crust is magnetized to depths up to a few tens of km. This contrasts strongly with the terrestrial seafloor, which acquires strong thermoremanance only in quenched basalt and sheeted dikes [5]. The magnetization imprint is controlled by the relative time scales of cooling and field reversals. Terrestrial divergent boundaries create new crust in regions of existing high heat flow. Here the brittle-ductile transition is relatively shallow, limiting the depth to which hydrothermal circulation can quickly cool intrusions (a 360˚C maximum temperature for effective hydrothermal circulation [6] is somewhat lower than the classical rock-mechanics BDT, but is consistent with the requirement that greater fracturing is developed for fluid circulation). Deeper, $\sqrt{t}$ conductive cooling is slower, and magnetic-field reversals at $<10^6$ year periods prevent acquisition of coherent thermoremanance. If crustal growth on Mars was able to occur with sufficient spatial heterogeneity such that new intrusions occurred into near-background heat flow (>60 mW/m^2 [7]), then the hydrothermal BDT may not have been reached until 15-20 km depth. Hydrothermal modeling (see below) indicates that large volumes of water at depth can circulate under these conditions and that $<10^5$ year is required to bring suggested typical martian magma chambers to below the curie temperature. The main field must maintain fixed polarity during this interval, so that developing thermoremanance is not scrambled.

Hydrothermal Circulation: The USGS HYDROTHERM [8] code and its GUI, HTpost [9], were used to run 2-D axisymmetric models of hydrothermal systems that exposed the magma chamber to porous host-rock across its entire surface. HYDROTHERM solves mass and energy balance equations for porous media flow via a finite-difference discretization and a Newton-Raphson iterative scheme. The modeling of steam and supercritical phases enables the code to handle temperatures in the range 0 to 1200°C and pressures in the range 0.5 to 10,000 bars.

We modeled magma chambers at depths from 2 to 15 km, volumes from 50 [10] to 2000 [11] km^3, aspect (diameter-to-height) ratios of 0.2, 2, and 20 emplaced in host-rock of permeabilities from 10^{-17} to 10^{-15} m^2. The permeability of the magma chamber is negligible when emplaced but increases to the host-rock value as it cools, simulating the development of secondary fracture porosity [6]. Due to the long period of time taken to complete models at high permeability and shallow depth, the geometry was scaled down and the discharge subsequently rescaled from similar models at lower permeability.

Our baseline model consisted of an instantaneously emplaced cylindrical magma chamber at 900°C, aspect ratio 2, and volume 50 km^3. The chamber was emplaced with its roof at a depth of 2 km and the surrounding host-rock was modeled to a depth of about 15 km, below which it was assumed to be impermeable. Pre-emplacement conditions in the host-rock were hydrostatic pressure and a geothermal gradient of 20°C/km. Host-rock permeability was 10^{-16} m^2 and porosity was 1%.

Comparison of aspect ratios. The flat, sill-like chamber (a.r. 20) produced the greatest peak discharge of the three models because of its large horizontal exposure (Fig. 2). The discharge dissipated more rapidly, however, because the chamber, having the greatest surface area to volume and being oriented perpendicular to the main flow direction, cooled more rapidly. Conversely, the tall, pipe-like chamber (a.r. 0.2) produced the shortest discharge peak but cooled more gradually, producing the greatest total discharge. Overall cooling times were greatest for the most equant

chamber because of its smallest surface area to volume ratio. Nonetheless, tenfold variations in aspect ratio produced changes in discharge of less than a factor of 2.

Permeability. For permeabilities between 10^{-17} and 10^{-15} m^2, discharge was roughly proportional to permeability, with decreasing rates for permeabilities higher than 10^{-15} m^2. Results from models similar to those of Gulick [10] in which an impermeable, thermally uncoupled chamber is exposed to host-rock of permeability 10^{-11} m^2 along its walls only, compared favorably. It was found that at lower permeabilities, discharge from this type of model produced a factor of 2.5 less discharge than our own fully coupled models.

Other Factors. Porosity did not significantly effect discharge for permeabilities greater than 10^{-16} m^2, implying that the porosity-velocity product is roughly constant. Discharge may be sharply reduced by a finite depth to the water table [12], which is not modeled in the homogeously saturated HYDROTHERM. Once water has reached the surface, some may be lost to other processes such as evaporation before doing any erosional work. Ice may also inhibit surface discharge.

Valley Networks: We estimated the discharge per km^2 produced by the valley networks to be between 2×10^6 and 5×10^9 m^3, based on an average valley density of 10^{-3}-10^{-2} km^{-1} [1], typical valley cross-section of 5000 by 100 m, and sediment-to-volume ratios of 4:1 to 1000:1 [10]. We computed the cumulative discharge from a continuous 15-km column of magma chambers that are assumed to intrude and cool separately. From the numerical models, we adopt a discharge radius of ten times the chamber radius, or about 25 km for the aspect-ratio 2, 50-km^3 chamber. The cumulative hydrothermal discharge is 10^{10} to 10^{12} m^3 for permeabilities between 10^{-17} to 10^{-15} m^2, whereas the valley-network discharge is 4×10^9 to 1×10^{13} m^3 over the same area. When integrated over the entire area of concentrated valley networks in Fig. 1 (1.8×10^7 km^2), the computed hydrothermal discharge is 2×10^{14} to 1×10^{16} m^3 and the estimated valley-network discharge is 4×10^{13} to 9×10^{16} m^3.

There are considerable uncertainties in these estimates. The effect of individual magma-chamber size and depth has not been fully explored. Various factors outlined above can limit the hydrothermal discharge to perhaps a few orders of magnitude lower than calculated. Conversely, the cumulative discharge over time would be larger as crust is added laterally as well as vertically. As the observed valley networks can preserve only the discharge at the end of heavy bombardment, it may be appropriate to consider creation of only part of the crust over this time. Nonetheless, a quantitative link between crustal formation, as recorded in the magnetic anomalies, and surficial discharge is suggested, and can be supported at large-scale permeabilities lower than previously suggested for Mars [10] or Earth [13].

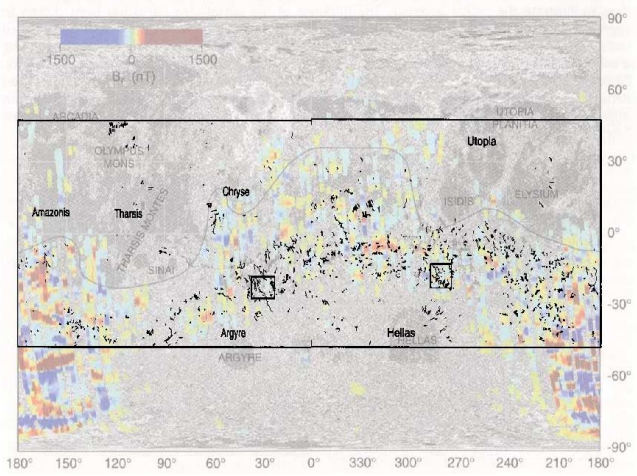

Figure 1. Magnetic anomalies [2] and valley networks [1]. Valley networks not included in this map [14], especially at longitudes close to 180°, also show significant correlation.

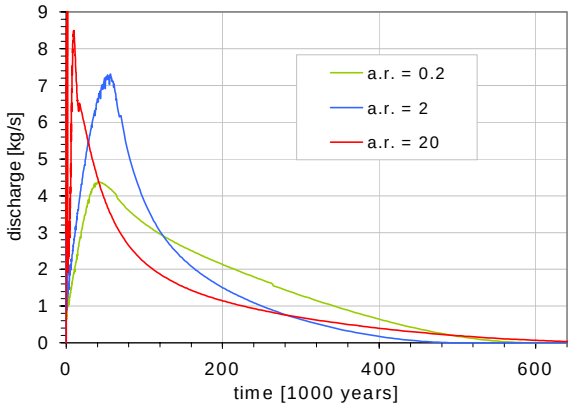

Figure 2. Total surficial discharge from models with three different magma chamber aspect ratios (a.r.). Early-time variations for a.r. = 20 are due to transient pressurization events.

References: [1] Carr M. H. (1996) *Water on Mars,* Oxford Univ. Press. [2] Acuña M. H. *et al* (1999), *Science, 284,* 790-793. [3] Connerney J. *et al* (1999), *Science*, *284*, 794-797. [4] Grimm, R.E. (2000), *LPSC XXXI,* #2056. [5] Keary P. and Vine F. J. (1990) *Global Tectonics*, Blackwell Sci. Pub., Oxford. [6] Hayba D. O. and Ingebritsen S. E. (1997), *JGR*, *102*, 12,235-12,252. [7] Schubert, G., et al. (1992), in *Mars*, Univ. Ariz. Press. [8] Hayba D. O. and Ingebritsen S. E. (1994), USGS Water-Res. Inv. Rep. 94-4045. [9] Hsieh P., *USGS*. [10] Gulick V. C. (1998) *JGR*, *103*, 19,365-19,387. [11] Head J. W. and Wilson L. (1994), *LPSC XXV*, 524. [12] Harrison K.T. and Grimm R.E. (1999) *LPSC XXX*, #1941. [13] Brace (1984), *JGR*, *89*, 4327-4330. [14] Carr M. H. and Clow G. D. (1981), *Icarus*, *48*, 91-117.